

7. S. Fukatsu, H. Yoshida, N. Usami, A. Fujiwara, Y. Takahashi, and Y. Shiraki, *Thin Solid Films*, **222**, 1 (1992).
8. S. Suzuki and T. Itoh, *J. Appl. Phys.*, **54**, 6385 (1983).
9. Y. Takahashi, H. Ishii, and K. Fujinaga, *Appl. Phys. Lett.*, **57**, 599 (1990).
10. H. Takasugi, M. Kawabe, and Y. Bando, *Jpn. J. Appl. Phys.*, **26**, L584 (1987).
11. H. L. Tsai and R. J. Matyi, *Appl. Phys. Lett.*, **55**, 265 (1989).
12. K. Fujinaga, Y. Takahashi, H. Ishii, I. Kawashima, and S. Hirota, *J. Vac. Sci. Technol.*, **B5**, 1551 (1987).
13. K. Fujinaga, *ibid.*, **B9**, 1511 (1991).
14. K. Fujinaga and K. Karasawa, *This Journal*, **140**, 2081 (1993).
15. R. People and J. C. Bean, *Appl. Phys. Lett.*, **47**, 322 (1985).
16. S. J. Rosner, S. M. Koch, and J. S. Harris, Jr., *ibid.*, **79**, 1764 (1986).
17. M. G. Norton, C. Scarfone, J. Li, B. Carter, and J. W. Mayer, *J. Mater. Res.*, **6**, 2022 (1991).
18. S. N. G. Chu, W. T. Tsang, T. H. Chiu, and A. T. Macrander, *J. Appl. Phys.*, **66**, 520 (1989).
19. J. W. Lee and H. L. Tsai, *J. Vac. Sci. Technol.*, **B5**, 819 (1987).

# Electron Spin Resonance Spectra of Silicon Dangling Bonds with Oxygen Back Bonds in Plasma-Deposited Amorphous SiO<sub>x</sub>

T. Inokuma, L. He, Y. Kurata, and S. Hasegawa

Department of Electrical and Computer Engineering, Faculty of Technology, Kanazawa University, Kanazawa 920, Japan

## ABSTRACT

Electron spin resonance (ESR) spectra in plasma-deposited amorphous SiO<sub>x</sub> films are investigated as a function of oxygen content,  $x$ . For  $x < 1.5$ , a broad resonance line around  $g = 2.005$  dominates the ESR spectra. On the other hand, for  $x > 1.5$ , several narrow lines become pronounced over the broad line. The narrow lines are assigned to arise from silicon dangling bond centers with  $\cdot\text{Si}=\text{Si}_2\text{O}$ ,  $\cdot\text{Si}=\text{SiO}_2$ , and  $\cdot\text{Si}=\text{O}_3$  configurations. The anisotropic  $g$  factors for the  $\cdot\text{Si}=\text{Si}_2\text{O}$  and  $\cdot\text{Si}=\text{SiO}_2$  centers are experimentally determined by means of a curve-fitting analysis. The  $g$  factors are also theoretically estimated on the basis of a molecular orbital calculation, and the values qualitatively agree with experimental ones. It is suggested that the broadening of the ESR line is reduced by the presence of an oxygen atom at the nearest-neighbor site of the trivalent silicon atom.

## Introduction

In metal-oxide-semiconductor (MOS) structures, an understanding of the defect structure at SiO<sub>2</sub>-Si interfaces is of growing importance because such defects are responsible for electrically active interface traps. Hence, these defects have been intensively studied by many research groups, and useful knowledge has been accumulated. In particular, electron spin resonance (ESR) studies combined with capacitance-voltage analyses have revealed that <111>-oriented silicon dangling bonds ( $P_b$  centers) at the interface are the microscopic origin of interface traps.<sup>1,2</sup> Further, Poindexter *et al.* have found a new paramagnetic center in oxidized Si (100) surfaces and speculatively assigned it to a silicon dangling bond with one oxygen neighbor ( $P_{b1}$  center).<sup>3</sup> Following that, the existence of a transition layer composed of various silicon suboxide states has been confirmed by photoelectron spectroscopy of thin oxidized layers.<sup>4</sup> However, very little is known about the characteristics of the silicon dangling bonds specific in the suboxide states. As for this subject, it should be helpful to investigate the fundamental properties of defects in silicon-oxygen alloys.

In this paper, we investigate the defects in amorphous (a-)SiO<sub>x</sub> films deposited using a plasma-enhanced chemical vapor deposition (PECVD) method. Since the PECVD method allows for growing silicon-oxygen alloys with any compositions between Si and SiO<sub>2</sub>, we can readily study the characteristics of defects in suboxide states which cannot be formed in an usual a-Si or a-SiO<sub>2</sub>. Using these silicon suboxide films, we focus on the ESR spectra of silicon dangling bond centers which have oxygen back bonds. The anisotropic  $g$  factors for the ESR centers in a-SiO<sub>x</sub> films are systematically analyzed as a function of the oxygen content,  $x$ , through both experimental and theoretical approaches. The results are discussed in connection with the structural and electronic properties of the ESR centers.

## Experimental

a-SiO<sub>x</sub> films were deposited by radio frequency (RF) plasma decomposition of an SiH<sub>4</sub>-O<sub>2</sub> mixture in a hot-wall-

type reactor. The RF power was inductively coupled to the mixture gas using a coil set outside the reactor tube. The RF power and its frequency were 10 W and 13.56 MHz, respectively. The flow rate ratio of O<sub>2</sub> to SiH<sub>4</sub> was varied from 0 to 1.8, under a fixed flow rate of SiH<sub>4</sub> at 1.8 sccm. The gas pressure and the deposition temperature in the reactor were maintained at 0.17 Torr and 300°C, respectively. Approximately 1 μm thick films were deposited simultaneously on Corning 7059 glass substrates for ESR measurements and on single-crystal Si for other measurements. Using electron probe microanalysis, the film composition  $x$  in SiO<sub>x</sub> was determined by comparing the intensities of Si Kα and O Kα signals with those for standards of high purity fused quartz (SiO<sub>2</sub>) and single-crystal Si. In these measurements, a well-known correction technique was used. The values of  $x$  were also estimated from the O 1s and Si 2p core level spectra in x-ray-induced photoelectron spectroscopy (XPS), using 500 Å thick films deposited on a single-crystal Si substrate.

The ESR spectra were measured using JOEL JEX-RE1X spectrometer operated at an X band frequency. The rather low microwave power 20 μW was used for minimizing the saturation effect on the signal intensity. The modulation amplitude of magnetic field was 0.01 mT. All the ESR measurements were performed at room temperature. The  $g$  values were calibrated using the value of the magnetic field at the halfway position between the third and fourth lines in six hyperfine lines for Mn<sup>2+</sup> ions in an MgO marker. The errors in the evaluation of  $g$  values are within 0.0001, as for their relative values.

## Experimental Results

Figure 1 shows the dependence of first-derivative ESR spectra for a-SiO<sub>x</sub> films on the film composition. The spectrum observed for  $x = 0$  (a-Si) consists of a broad line at  $g = 2.0055$ , and is attributed to silicon dangling bonds with a  $\cdot\text{Si}=\text{Si}_3$  configuration ( $D$  center). The main cause of the broad resonance line is generally considered to arise from anisotropy of the  $g$  factor. In addition, the structural fluctuation in the vicinity of the dangling bonds also con-

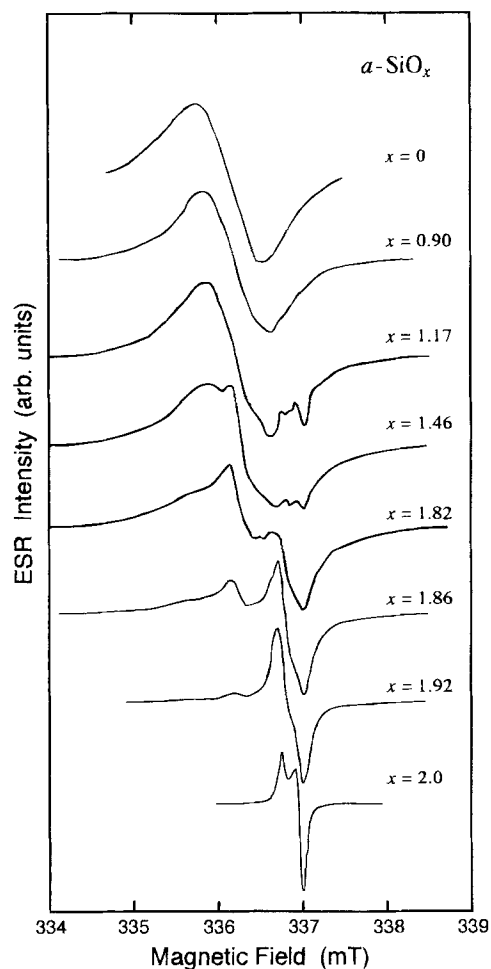


Fig. 1. Dependence of ESR spectra in  $a\text{-SiO}_x$  films on the oxygen content  $x$ .

tributes to an inhomogeneous broadening of the resonance line.<sup>5</sup> On the other hand, the sharp spectrum observed for  $x = 2.0$  ( $a\text{-SiO}_2$ ) shows the characteristics of  $E'$  centers that is an intrinsic defect center in irradiated silica. The origin of  $E'$  centers is essentially a silicon dangling bond with a  $\cdot\text{Si}=\text{O}_3$  configuration. The numerous types of  $E'$  centers, which are caused by differences in additional structures to  $\cdot\text{Si}=\text{O}_3$  bonding units, have been reported up to the present.<sup>6</sup>

As seen in Fig. 1, for  $x < 1.5$ , the narrow lines are weak, and merely give a small distortion to the broad  $D$  center signal. On the other hand, for  $x > 1.5$  several narrow lines are observed besides  $D$  and  $E'$  center signals, and the narrow lines become pronounced with increasing  $x$ . Thus, the spectra drastically changes in this composition range. The narrow lines would arise from silicon dangling bonds with one or more oxygen back bond(s).<sup>7,8</sup>

To analyze these complicated ESR spectra, we decomposed it into several elemental components. In the decomposition procedure of the spectra, we assumed four spectral components which correspond to  $\cdot\text{Si}=\text{Si}_{3-n}\text{O}_n$  ( $n = 0, 1, 2,$  or  $3$ ) dangling bond centers. For the  $\cdot\text{Si}=\text{Si}_3$  center, a single isotropic  $g$  factor and Lorentzian line shape were adequate to reproduce the signal. A typical ESR center having  $\cdot\text{Si}=\text{Si}_3$ -type configurations is the  $D$  center with an isotropic  $g$  value around  $g = 2.0055$ . Further, the  $P_b$  center with anisotropic  $g$  values of  $g_{\parallel} = 2.0012$  and  $g_{\perp} = 2.0082$ , which exist at  $\text{SiO}_2\text{-Si}$  interface, also has  $\cdot\text{Si}=\text{Si}_3$ -type configurations. However, it was perceived that smeared powder patterns using the anisotropic  $g$  values, which will be described later, cannot reproduce the experimental spectra correctly. Therefore, we assumed the isotropic  $g$  factor for the  $\cdot\text{Si}=\text{Si}_3$  center, attaching importance to the reproduction of the observed spectra. With increasing  $x$ , the zero

crossing  $g$  value for the  $\cdot\text{Si}=\text{Si}_3$  center decreased from 2.0055 to 2.0051 over the composition range of  $x < 0.2$ , but it seems to remain unchanged for  $x > 0.2$ . For  $\cdot\text{Si}=\text{Si}_3\text{O}$  center, the  $g$  values of  $E'$  centers,  $g_{\parallel} = 2.0018$  and  $g_{\perp} = 2.0003$ , were applicable. The  $E'$  center has been believed to be a simple isolated  $\cdot\text{Si}=\text{O}_3$  center. In order to extract the spectral components due to  $\cdot\text{Si}=\text{Si}_2\text{O}$  and  $\cdot\text{Si}=\text{SiO}_2$  centers from the observed spectra, we examined each of the components by a curve-fitting analysis to reproduce the experimental spectra consistently. Consequently, it was found that we must take into account the anisotropy of  $g$  factors for the  $\cdot\text{Si}=\text{Si}_2\text{O}$  and  $\cdot\text{Si}=\text{SiO}_2$  centers, as is the case for the  $\cdot\text{Si}=\text{O}_3$  center. To involve effects of the  $g$  anisotropy in a simulated ESR spectrum, we used a powder pattern  $P(g)$  that describes the resonance intensity for a given value of  $g$ , as given by

$$P(g) = \frac{1}{4\pi} \int_{\Omega} \delta(g_0(\theta, \varphi) - g) \sin \theta d\theta d\varphi \quad [1]$$

where,  $g_0(\theta, \varphi)$  denotes the angular dependence of  $g$  under a spherical coordinate system, *i.e.*

$$g_0(\theta, \varphi) = \sqrt{g_1^2 \cos^2 \theta + g_2^2 \sin^2 \theta \cos^2 \varphi + g_3^2 \sin^2 \theta \sin^2 \varphi} \quad [2]$$

Here, the parameter  $g_1$ ,  $g_2$ , and  $g_3$  are the principal  $g$  values. The integration in Eq. 1 is done over all directions  $\Omega$ . The  $\delta(x)$  denotes Dirac's delta function. After  $g$  in Eq. 1 was converted to magnetic field under conditions of a fixed microwave frequency, the function of  $P(g)$  was smeared by convolution with a Lorentzian function with a broadening factor  $\gamma$ , *i.e.*

$$L(H) = \frac{\gamma}{\pi} \frac{1}{H^2 + \gamma^2} \quad [3]$$

The first-derivative spectra of the four components and the parameters  $g$  and  $\gamma$ , which were used to simulate the experimental spectra, are shown by the solid lines in Fig. 2. As a comparison of the isotropic spectrum for the  $\cdot\text{Si}=\text{Si}_3$  center, an example of the spectrum using the anisotropic  $g$  values of the  $P_b$  center is also shown in Fig. 2 by a broken line; it was not used in the curve-fitting analysis. The intensities of their respective components and the dependence on the oxygen content were evaluated by fitting the sum of the above calculated components to the experimental spectra. The values of  $g$  and  $\gamma$  for the individual components were always fixed through the fitting operation. In Fig. 3, typical results of the curve fitting are displayed for three different films. We can see a good agreement between the experimental spectra and the fitted lines.

Figure 4 shows the variation of relative intensities for the four spectral components as a function of  $x$ . Since the broad signal due to  $\cdot\text{Si}=\text{Si}_3$  center dominates the spectrum for  $x < 1.5$  as shown in Fig. 1, signals due to other centers were not clearly distinguishable from that of the  $\cdot\text{Si}=\text{Si}_3$  center. Therefore, the composition range of the plots in Fig. 4 was limited in  $1.3 < x < 2.0$ . As  $x$  increases, the principal component contributing to the observed spectra changes from the  $\cdot\text{Si}=\text{Si}_3$  center to the  $\cdot\text{Si}=\text{Si}_2\text{O}$ ,  $\cdot\text{Si}=\text{SiO}_2$ , and  $\cdot\text{Si}=\text{O}_3$  centers in turn. Furthermore, the relative intensity of each component drastically changes in a narrow range of  $x = 1.8\text{-}2.0$ . This composition range is considerably higher than a statistical prediction for the probability of occurrence of  $\text{Si}(\text{Si}_3\text{O})$ ,  $\text{Si}(\text{Si}_2\text{O}_2)$ , and  $\text{Si}(\text{SiO}_3)$  tetrahedra, *i.e.*, the random bonding model (RBM). Whereas, results of Si 2p core-level spectra<sup>9,10</sup> and Si-H vibrational spectra<sup>11</sup> have suggested that a change in the bonding configuration as a function of  $x$  obeys the RBM, showing a striking contrast to the result shown in Fig. 4.

The total spin density  $N_s$  as a function of  $x$  is plotted in Fig. 5. As the oxygen content increases,  $N_s$  rapidly increases over the range of both  $x = 0$  to  $0.3$  and  $x = 1.4$  to  $1.8$ , while it gradually increases for  $x = 0.3$  to  $1.4$ . Above  $x = 1.8$ ,  $N_s$  decreases again.

### Theoretical Analysis

Previously, Holzenkämpfer *et al.*<sup>7</sup> have analyzed the ESR spectra after He<sup>+</sup> ion irradiation of a-SiO<sub>x</sub> films deposited by electron beam evaporation. In that analysis, they have assumed isotropic *g* factors for every type of the silicon dangling bond centers with oxygen back bonds. However, selection of the spectral components used seemed rather tentative, and its physical basis is unclear. In the present analysis of the ESR spectra, the anisotropy of the *g* factor is required for reproducing the observed spectra. We present the results of a theoretical analysis with respect to an effect of back bonded oxygens on the *g* factor of silicon dangling bond centers.

For calculating the *g* tensor of a given paramagnetic center, it is required to know at the outset the electronic structure for the center. As a model of the bonding structure determining the electronic structure for the silicon dangling bonds in a-SiO<sub>x</sub>, we presumed small clusters illustrated in Fig. 6. In these clusters, hydrogen atoms are attached to the unsaturated bonds so as to satisfy the valence requirement, except for an Si atom bearing a dangling bond. The electronic structures of those clusters were calculated by the PM3 method<sup>12</sup> using MOPAC Ver. 6, which is a program for self-consistent semiempirical molecular orbital calculation. In this method, Slater-type atomic orbitals of valence electrons are used as the basis set. The MNDO-PM3 Hamiltonian, which involves empirical parameters in the core-core repulsion term, is applied to the molecular orbital calculation. Since the clusters shown in Fig. 6 include an unpaired electron, we performed a spin-unrestricted calculation that allows a molecular orbital to have an independent energy and wave function for

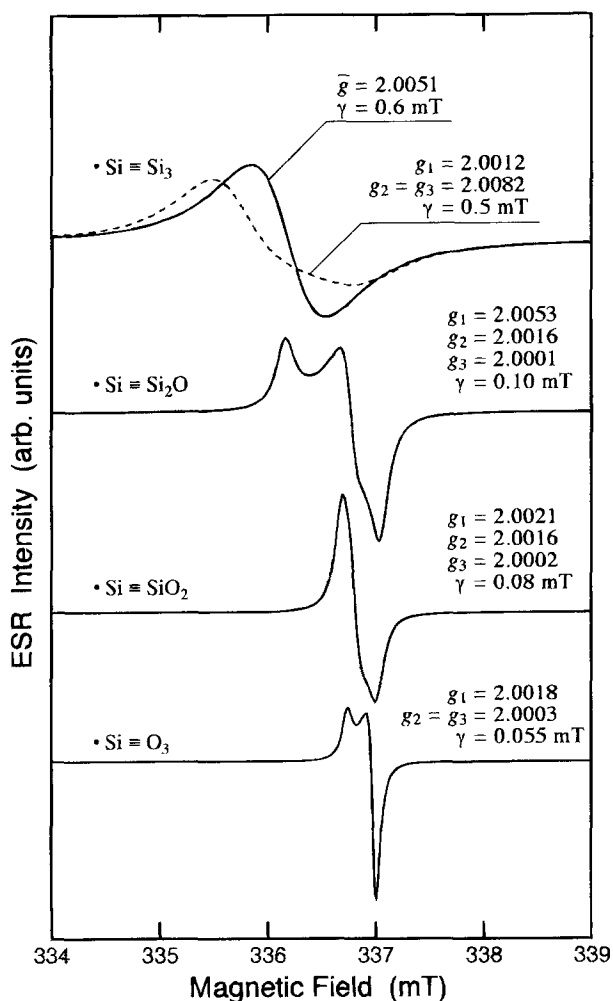


Fig. 2. ESR spectral components used to simulate the experimental spectra.

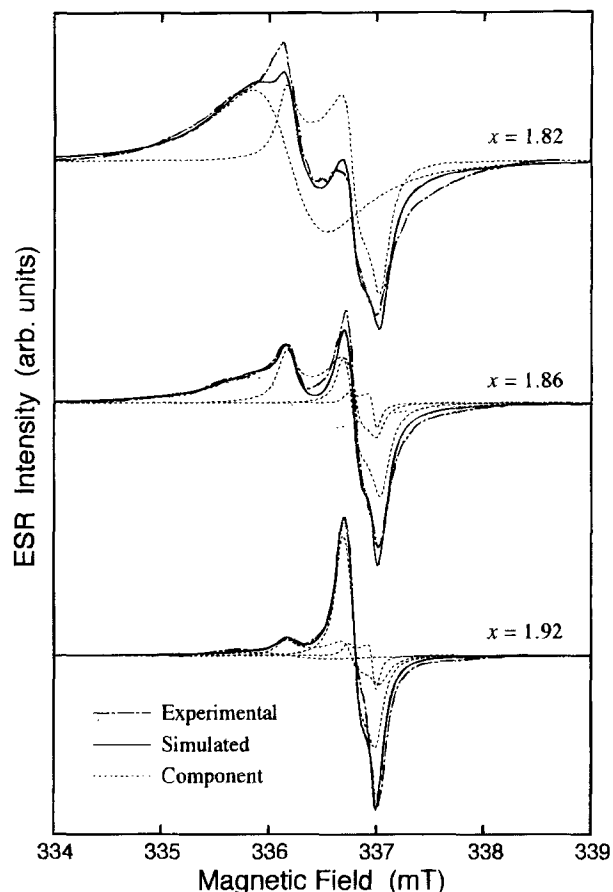


Fig. 3. Typical results of the fittings of simulated spectra on experimental ones.

$\alpha$ -spin-occupied and  $\beta$ -spin-occupied states. The atomic geometry was adjusted so as to minimize the energy of formation of the cluster by employing the Broyden-Fletcher-Goldfarb-Shanno optimizer routine<sup>13</sup> included in the MOPAC program.

For all the clusters, *sp*-hybridized dangling bond orbitals were formed on the trivalent Si atoms. The energy levels of the dangling bond states were located between the

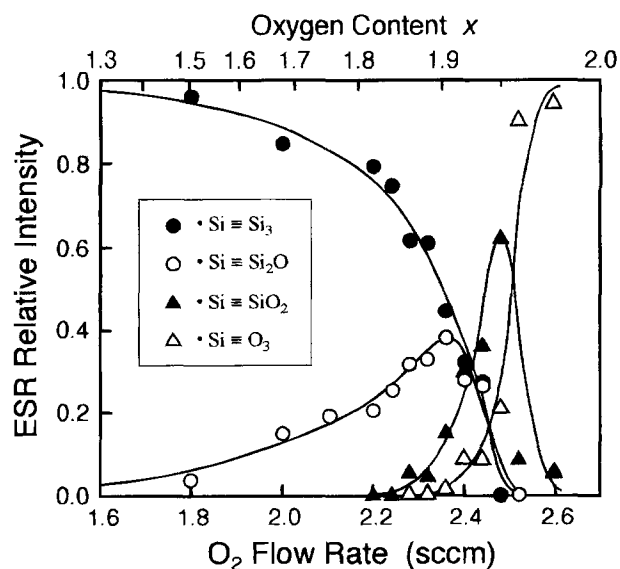


Fig. 4. Dependence of relative intensities of the spectral components on the O<sub>2</sub> flow rate during the film deposition. The upper abscissa indicates an approximate content *x* of oxygen atoms in the film.

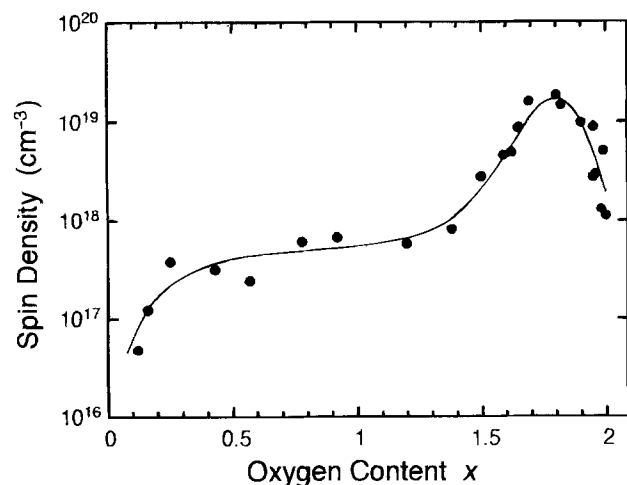


Fig. 5. Dependence of the ESR signal intensity  $N_e$  on the oxygen content  $x$ .

highest doubly occupied level and the lowest unoccupied level. The characteristics of the dangling bond states are summarized in Table I. It is found that formation of the oxygen back bonds shifts the energy level of the dangling bond state upward. This result agrees well with that reported by Beltran.<sup>14</sup> As seen in Table I, the unpaired electron on the trivalent Si atom has 60 ~ 80% on-site localization, and which depends on the back-bonded species. From the values of s-to-p ratio,  $\chi$ , in Table I, one can find that the contribution of 3s atomic orbital in the trivalent Si atom to the dangling bond orbital increases from 8% for the  $\cdot\text{Si}=\text{Si}_3\text{H}_9$  center to 33% for the  $\cdot\text{Si}=\text{O}_3$  center. These values agree well with those found experimentally through the analyses of  $^{29}\text{Si}$  hyperfine ESR signals for a-Si:H and a-SiO<sub>2</sub>; the ratio of s orbital component in the dangling bond orbital is ~10% for the D center<sup>15,16</sup> and ~24% for the E' center.<sup>17,18</sup>

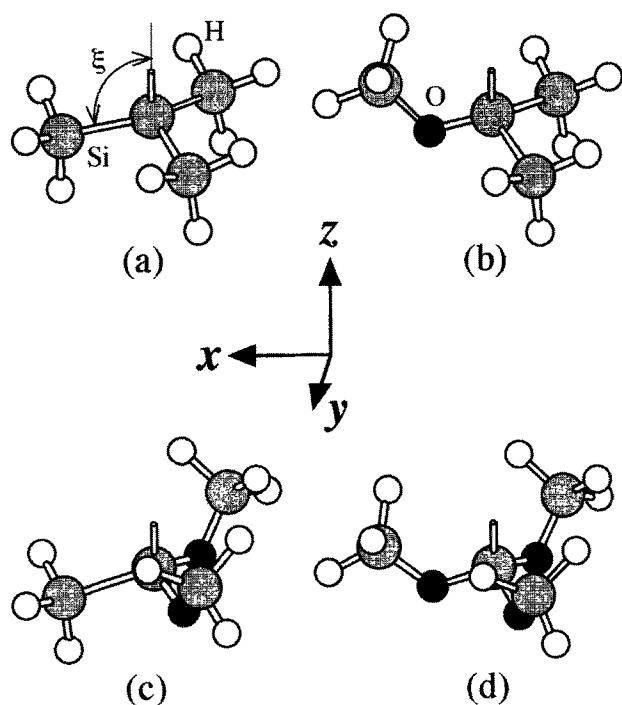


Fig. 6. (a)  $\cdot\text{Si}=\text{Si}_3\text{H}_9$ , (b)  $\cdot\text{Si}=\text{Si}_2(\text{OSi})\text{H}_9$ , (c)  $\cdot\text{Si}=\text{Si}(\text{OSi})_2\text{H}_9$ , and (d)  $\cdot\text{Si}=(\text{OSi})_3\text{H}_9$  clusters used to calculate the electronic structures of the silicon dangling bond centers in a-SiO<sub>x</sub> films. Equilibrium atomic geometries as a result of the calculation are illustrated. The  $x$ ,  $y$ , and  $z$  axes indicate the rectangular coordinate system used in the calculation.

Table I. Characteristics of the dangling bond centers obtained by a molecular orbital calculation for the clusters in Fig. 6.  $E_{\text{DB}}$  is the energy of the singly occupied state relative to the vacuum level,  $\rho$  the percentage localization of the unpaired electron at the trivalent Si atom, and  $\chi$  the relative contribution of p orbitals when the sp hybridization of the dangling bond orbital is expressed as  $sp^\chi$ .  $q$  is the additional partial charge on the trivalent Si atom.  $\xi_{\text{MO}}$  is the bond angles of the back bonds for the equilibrium geometry of the cluster and  $\xi_e$  is obtained using Eq. 4.

| Cluster  | $E_{\text{DB}}$ (eV) | $\rho$ (%) | $\chi$ | $q$     | $\xi_{\text{MO}}$ (°) | $\xi_e$ (°) |
|--|----------------------|------------|--------|---------|-----------------------|-------------|
| $\cdot\text{Si}=\text{Si}_3\text{H}_9$             | -7.9                 | 78         | 11.2   | -0.04 e | 102.3                 | 101.4       |
| $\cdot\text{Si}=\text{Si}_2(\text{OSi})\text{H}_9$ | -7.3                 | 69         | 5.0    | +0.31 e | 104 <sup>a</sup>      | 106.1       |
| $\cdot\text{Si}=\text{Si}(\text{OSi})_2\text{H}_9$ | -6.7                 | 61         | 2.9    | +0.57 e | 106 <sup>a</sup>      | 109.7       |
| $\cdot\text{Si}=(\text{OSi})_3\text{H}_9$          | -6.5                 | 69         | 2.0    | +0.78 e | 108.8                 | 112.2       |

<sup>a</sup> The angles  $\xi_{\text{MO}}$  for the  $\cdot\text{Si}=\text{Si}_2(\text{OSi})\text{H}_9$  and  $\cdot\text{Si}=\text{Si}(\text{OSi})_2\text{H}_9$  clusters are the averaged values, because the three back bonds are not equivalent.

If the value of  $\chi$  depends only on the geometry of a silicon dangling bond center, the relationship between  $x$  and the bond angle  $\xi$  (see Fig. 6) can be expressed as

$$\tan \xi = -\{2[1 + \chi]\}^{1/2} \quad [4]$$

Since the unpaired electron in the  $\cdot\text{Si}=\text{Si}_3\text{H}_9$  cluster exhibits a strong p character ( $\chi = 11.2$ ), the trivalent Si atom should move vertically toward the plane formed by the three back bonded Si atoms, against its normal position expected in  $sp^3$  configurations. Furthermore, the value of  $\chi$  along with Eq. 4 indicates that the trivalent Si atom is gradually protruded from the above-mentioned plane with increasing the number of oxygen neighbors, as shown in Table I, whereas Edwards and Fowler have pointed out that the values of  $\chi$  depend not only on the geometry of the defect but also on the partial charge existing on the defect atom.<sup>19</sup> According to the present calculation, the trivalent Si atom becomes positively charged as O atoms are bonded to the Si atom (see Table I). This is consistent with the fact that the oxygen atom is most electronegative within the constituent Si, H, and O atoms. Further, since the Si 3s orbital lies below the 3p orbitals in energy, an increase in the positive charge on the trivalent Si atom should lead to an increase in the relative contribution of the s character in the dangling bond orbital, that is, a decrease in  $\chi$ . This, in turn, means that increased positive charge on the trivalent Si atom overestimates the value of  $\xi$  which is calculated using Eq. 4. As shown in Table I, this overestimation can be seen as the difference between the values of  $\xi_{\text{MO}}$  and  $\xi_e$ .

Using the results of the molecular orbital calculation, the  $g$  tensors of dangling bond centers in a given cluster can be calculated. Provided that the molecular orbitals of all the states are confined in the cluster, the  $g$  tensor is given by<sup>20</sup>

$$g_{ij} = g_e \delta_{ij} - 2\lambda \sum_{n \neq 0} \frac{\langle \phi_0 | L_i | \phi_n \rangle \langle \phi_n | L_j | \phi_0 \rangle}{E_n - E_0} \quad [5]$$

where  $g_e = 2.0023$  is the  $g$  value of free electron,  $\lambda$  the spin-orbit coupling constant,  $L_i$  the orbital angular momentum operators, and  $i$  and  $j$  denote the  $x$ ,  $y$ , or  $z$  axes in a rectangular coordinate, respectively.  $E_0$  and  $\phi_0$  are, respectively, the energy and the molecular orbital of the dangling bond state.  $E_n$  and  $\phi_n$  are those of the doubly occupied and unoccupied states that may be regarded as valence- and conduction-band states in a sense. As  $\phi_0$  and  $\phi_n$ , we take the components of the atomic orbitals at the trivalent Si site for simplification. The value of 0.019 eV was used as the spin-orbit coupling constant for silicon.<sup>21</sup> The principal values of the  $g$  tensors obtained for each of the clusters are shown in Table II. For all the clusters, the direction of the principal axes of the  $g$  tensor orientates approximately along the coordinate axes indicated in Fig. 6.

## Discussion

We showed that the average  $g$  value of a silicon dangling bond center is reduced with an increase in oxygen neigh-

bors. According to the molecular orbital calculation, the energy,  $E_{DB}$ , of electrons in dangling bond states increases with increasing the number of oxygen neighbors as shown in Table I. As expected from Eq. 5, a reduction of the  $g$  value would be caused by the increase of  $E_{DB}$  that corresponds to  $E_0$  in Eq. 5. Thus, the upward shift of  $E_{DB}$  roughly explains the overall variation of the  $g$  value accompanied with a change in the back-bonded species. Furthermore, the  $g$  shift would decrease as the magnitude of  $\langle \phi_0 | L_i | \phi_n \rangle < \phi_n | L_i | \phi_0 \rangle$  in Eq. 5 decreases. This is the case that the contribution of the  $p$  orbitals in the dangling bond orbital  $\phi_0$  decreases with increasing the number of oxygen neighbors.

When the  $g$  values in Fig. 2 and those in Table II are compared, it is found that individual values of the principal  $g$  values obtained theoretically are considerably different from those determined through the fitting procedure of the experimental spectra. So the results for the principal  $g$  values obtained theoretically are not so sufficient as to perform the quantitative analysis. However, it does allow the qualitative analysis based on the relationship between the direction of the principal axes and the magnitude of the  $g$  shifts. By comparing the theoretically determined  $g$  tensors with the experimental ones, we can determine the direction of principal axes for each value of  $g$  obtained experimentally. For the  $\cdot\text{Si}=\text{Si}_2\text{O}$  center, the result of the calculation suggest  $g_{xx} > g_{yy} \sim g_{zz}$  thus no obvious difference appeared between  $g_{yy}$  and  $g_{zz}$  in our calculation. On the other hand, three kinds of  $g$  values extracted experimentally were clearly distinguishable. To establish the correlations between the experimental and theoretical  $g$  values, we invoked the tendency that a dangling bond exhibits a smaller  $g$  shift as the principal axis is parallel to the direction of the dangling orbital. Accordingly, the value  $g_2 = 2.0016$  is more likely to be assigned to  $g_{zz}$  than  $g_{yy}$ . Thus the principal  $g$  values may be assigned as  $g_{xx} = 2.0053$ ,  $g_{yy} = 2.0001$ , and  $g_{zz} = 2.0016$ . For the  $\cdot\text{Si}=\text{SiO}_2$  center,  $g_{xx} = 2.0002$ ,  $g_{yy} = 2.0021$ , and  $g_{zz} = 2.0016$  are suggested by adopting the order in the magnitude for the  $g$  values obtained theoretically.

In Fig. 2, the line broadening factor,  $\gamma$ , is found to be reduced as oxygen back bonds exist. Note that the spectral component assumed for the  $\cdot\text{Si}=\text{Si}_3$  center is based on an isotropic  $g$  value, in contrast with other three components. Therefore, we cannot straightforwardly compare the value of  $\gamma = 0.06$  mT for the  $\cdot\text{Si}=\text{Si}_3$  center with those for other centers. However, even if the anisotropic  $g$  factor of the  $P_b$  center was used for reproducing the spectrum for the  $\cdot\text{Si}=\text{Si}_3$  center, a value of  $\gamma \sim 0.5$  mT would be required to obtain a spectrum rather similar to the observed one (see Fig. 2). The value of 0.5 mT is still larger than the values of 0.05 to 0.10 mT for the oxygen-back-bonded centers. Thus, it is unambiguous that even one oxygen neighbor of a trivalent Si atom brings about a remarkable reduction of the broadening factor.

In amorphous materials, the  $g$  value distribution arising from structural fluctuation contributes to a significant part of the ESR line broadening.<sup>22</sup> Therefore, the smaller  $\gamma$  for the  $\cdot\text{Si}=\text{Si}_2\text{O}$  centers than that for the  $\cdot\text{Si}=\text{Si}_3$  center suggests that, for the  $\cdot\text{Si}=\text{Si}_2\text{O}$  center, the structural fluctuation is less effective to the distribution of  $g$  values, or that the fluctuation itself is smaller. To examine effects of the structural fluctuation on the  $g$  factors, we theoretically estimated the change in  $g$  values arising from a change in the bond angles of the back bonds. The method used here is the same as that described in the previous section, with the exception that the bond angles of the three back bonds

were fixed (not optimized) in the molecular orbital calculation. When the bond angles  $\xi$  is varied simultaneously by  $\pm 2^\circ$  around their equilibrium values, the averaged changes in the  $g$  values are 0.00029, 0.00024, 0.00012, and 0.00008 for the  $\cdot\text{Si}=\text{Si}_3\text{H}_3$ ,  $\cdot\text{Si}=\text{Si}_2(\text{OSi})\text{H}_3$ ,  $\cdot\text{Si}=\text{Si}(\text{OSi})_2\text{H}_3$ , and  $\cdot\text{Si}=(\text{OSi})_3\text{H}_3$  clusters, respectively. According to this estimation, the sensitivity of the  $g$  factors to the variation of local structure seems to exhibit no abrupt dependence on the number of oxygen neighbors. Therefore, the remarkable difference between the spectral widths for the  $\cdot\text{Si}=\text{Si}_3$  and  $\cdot\text{Si}=\text{Si}_2\text{O}$  centers can be attributed to the difference in magnitude of the fluctuation in the local structure; the structural fluctuation in the  $\cdot\text{Si}=\text{Si}_2\text{O}$  centers is considered to be smaller than that in the  $\cdot\text{Si}=\text{Si}_3$  centers.

As shown in Fig. 4, the relative intensities of the four spectral components drastically change in a narrow range of  $1.8 < x < 2.0$ , while that for the  $\cdot\text{Si}=\text{Si}_3$  center dominate the ESR spectra of  $x < 1.8$ . To discuss this result in relation to the relative density of the defects in the films, we must take into account the electron transfers between the dangling bond centers which have different numbers of oxygen neighbors. If the transfer of electrons occurs in the present films, paramagnetic, neutral dangling bonds would be converted into diamagnetic, charged dangling bonds. Since the latter centers cannot be detected by ESR measurements, the electron transfer should affect the relative intensity of ESR signals.

Whether the electron transfer occurs or not is closely related to the relative location of the energy level of the dangling bond state and to the effective correlation energy  $U_{\text{eff}}$ .  $U_{\text{eff}}$  is defined as the energy required to form the doubly occupied dangling bond state ( $D_n^-$ ) from the singly occupied one ( $D_n$ ), where the  $D_n$  and  $D_n^-$  states describe neutral- and negatively charged states of the dangling bonds in  $\cdot\text{Si}=\text{Si}_3$  the electron transfer from the  $D_n$  state to the  $D_0$  state, respectively. If the energy levels of the  $D_n$  states with  $n \geq 1$  lay lower than the level of the  $D_0$  state, which results in  $D_0$  states, would not occur. However, according to the present calculation, the level of the  $D_n$  states with  $n \geq 1$  are suggested to lie at locations higher than at least 0.6 eV compared with the  $D_0$  state (see Table I). Since this energy difference of 0.6 eV is larger than the value of  $U_{\text{eff}} = 0.2$  to 0.3 eV for the  $D$  center observed in nondoped a-Si:H films,<sup>23,24</sup> it is possible that the electron transfer from the  $D_n$  states with  $n \geq 1$  to the  $D_0$  state. In this case, as far as the  $\cdot\text{Si}=\text{Si}_3$  center exists with a larger density than the oxygen-back-bonded centers, the signal from the oxygen-back-bonded centers should be suppressed. Therefore, if the effect of the electron transfer is considered, it can be stated that the density of  $\cdot\text{Si}=\text{Si}_3$  center is dominant up to  $x \sim 1.8$ , i.e., the  $\cdot\text{Si}=\text{Si}_3$  configuration are formed even in the a-SiO<sub>x</sub> films for  $x \sim 1.8$ . Within the RBM, in contrast, the probability for the formation of the  $\cdot\text{Si}=\text{Si}_3$  configurations is expected to be very small for  $x > 1.5$  in a-SiO<sub>x</sub>. Also in experiments, the bonding configuration of a-SiO<sub>x</sub> systems has been confirmed to obey the RBM, basically.<sup>9,10</sup> The result in Fig. 4 provides a limitation of the simple statistical approach as to the probability of defect formation in the a-SiO<sub>x</sub> system. The discrepancy between the ESR result and the RBM may be due to the fact that defects are minor structural components.

## Conclusion

We have studied the ESR spectra in plasma-deposited amorphous SiO<sub>x</sub> films as a function of oxygen content  $x$ . For  $x < 1.5$ , a broad resonance line similar to the spectrum for a-Si:H dominates the ESR spectra, and which was attributed to silicon dangling bond centers with a  $\cdot\text{Si}=\text{Si}_3$  configuration. The narrow lines, which became pronounced over the broad line for  $x > 1.5$ , were assigned to the signal arising from silicon dangling bond centers with  $\cdot\text{Si}=\text{Si}_2\text{O}$ ,  $\cdot\text{Si}=\text{SiO}_2$ , and  $\cdot\text{Si}=\text{O}_3$  configurations. The anisotropic  $g$  factors for the  $\cdot\text{Si}=\text{Si}_2\text{O}$  and  $\cdot\text{Si}=\text{SiO}_2$  centers were successfully determined by means of a curve fitting analysis. The values of  $g$  factors which were obtained theo-

**Table II. The principal  $g$  values calculated using the results of the molecular orbital calculation and Eq. 5.**

| Cluster  | $g_{xx}$ | $g_{yy}$ | $g_{zz}$ |
|--|----------|----------|----------|
| $\cdot\text{Si}=\text{Si}_3\text{H}_3$             | 2.0074   | 2.0074   | 2.0023   |
| $\cdot\text{Si}=\text{Si}_2(\text{OSi})\text{H}_3$ | 2.0059   | 2.0023   | 2.0023   |
| $\cdot\text{Si}=\text{Si}(\text{OSi})_2\text{H}_3$ | 2.0015   | 2.0028   | 2.0023   |
| $\cdot\text{Si}=(\text{OSi})_3\text{H}_3$          | 2.0016   | 2.0016   | 2.0023   |

retically using a molecular orbital calculation provided qualitative agreement with the experimental ones. It was suggested that the structural fluctuation in the vicinity of the silicon dangling bonds is reduced by the presence of an oxygen back bond. The composition dependence of relative intensity of the components, which were obtained through the curve fitting analysis, suggested that the  $\cdot\text{Si}\equiv\text{Si}_3$  configuration exists with a considerable density in the  $\alpha\text{-SiO}_x$  films for  $x \sim 1.8$ .

### Acknowledgments

This work has been partially supported by Grant-In-Aid 05650009 for Scientific Research from Ministry of Education, Science and Culture.

Manuscript submitted Oct. 19, 1994; revised manuscript received March 22, 1995.

Kanazawa University assisted in meeting the publication costs of this article.

### REFERENCES

1. Y. Nishi, *Jpn. J. Appl. Phys.*, **10**, 52 (1971).
2. P. J. Caplan, E. H. Poindexter, B. E. Deal, and R. R. Razouk, *J. Appl. Phys.*, **50**, 5847 (1979).
3. E. H. Poindexter, P. J. Caplan, B. E. Deal, and R. R. Razouk, *ibid.*, **52**, 879 (1981).
4. F. J. Himpsel, F. R. McFeely, A. Tareb-Ibrahimi, J. A. Yarmoff, and G. Hollinger, *Phys. Rev. B*, **38**, 6084 (1988).
5. R. A. Street and D. K. Biegelsen, in *The Physics of Hydrogenated Amorphous Silicon II*, J. D. Joannopoulos and G. Lucovsky, Editors, pp. 251-208, Springer-Verlag, Berlin (1984).
6. W. L. Warren, E. H. Poindexter, M. Offenberger, and W. Muller-Warmuth, *This Journal*, **139**, 872 (1992).
7. E. Holzenkämpfer, F.-W. Richter, J. Stuke, and U. Voget-Grote, *J. Non-Cryst. Solids*, **32**, 327 (1979).
8. S. Otsubo, M. Saito, A. Morimoto, M. Kumeda, and T. Shimizu, *Jpn. J. Appl. Phys.*, **27**, L1999 (1988).
9. F. G. Bell and L. Ley, *Phys. Rev.*, **37**, 8383 (1988).
10. S. Hasegawa, L. He, T. Inokuma, and Y. Kurata, *Phys. Rev. B*, **46**, 12478 (1992).
11. L. He, Y. Kurata, T. Inokuma, and S. Hasegawa, *Appl. Phys. Lett.*, **63**, 162 (1993).
12. J. J. P. Stewart, *J. Comput. Chem.*, **10**, 221 (1989).
13. D. F. Shanno, *J. Optim. Theory Appl.*, **46**, 87 (1985).
14. M. R. Beltran, *J. Non-Cryst. Solids*, **163**, 148 (1993).
15. D. K. Biegelsen and M. Stutzmann, *Phys. Rev. B*, **33**, 3006 (1986).
16. M. Stutzmann and D. K. Biegelsen, *Phys. Rev. Lett.*, **60**, 1682 (1988).
17. R. H. Silsbee, *J. Appl. Phys.*, **32**, 1459 (1961).
18. D. L. Griscom, E. J. Friebele, and G. H. Sigel, Jr., *Solid State Commun.*, **15**, 479 (1974).
19. A. H. Edwards and W. B. Fowler, *Phys. Rev. B*, **41**, 10816 (1990).
20. M. H. L. Plyce, *Proc. Phys. Soc.*, **A63**, 25 (1950).
21. N. Ishii, M. Kumeda, and T. Shimizu, *Jpn. J. Appl. Phys.*, **20**, L673 (1981).
22. D. L. Griscom, *J. Non-Cryst. Solids*, **31**, 241 (1978).
23. M. Stutzmann and J. Stuke, *Solid State Commun.*, **47**, 635 (1983).
24. K. Hattori, H. Okamoto, and Y. Hamakawa, *Philos. Mag. B*, **57**, 13 (1988).